

# PCCP

Accepted Manuscript



This is an *Accepted Manuscript*, which has been through the Royal Society of Chemistry peer review process and has been accepted for publication.

*Accepted Manuscripts* are published online shortly after acceptance, before technical editing, formatting and proof reading. Using this free service, authors can make their results available to the community, in citable form, before we publish the edited article. We will replace this *Accepted Manuscript* with the edited and formatted *Advance Article* as soon as it is available.

You can find more information about *Accepted Manuscripts* in the [Information for Authors](#).

Please note that technical editing may introduce minor changes to the text and/or graphics, which may alter content. The journal's standard [Terms & Conditions](#) and the [Ethical guidelines](#) still apply. In no event shall the Royal Society of Chemistry be held responsible for any errors or omissions in this *Accepted Manuscript* or any consequences arising from the use of any information it contains.

## Choosing a Density Functional for Modeling Adsorptive Hydrogen Storage: Reference Quantum Mechanical Calculations and a Comparison of Dispersion-Corrected Density Functionals

Mikuláš Kocman<sup>1</sup>, Petr Jurečka<sup>1,\*</sup>, Matúš Dubecký<sup>1</sup>, Michal Otyepka<sup>1</sup>, Yeonchoo Cho<sup>2,3</sup>, Kwang S. Kim<sup>4</sup>

<sup>1</sup> Regional Centre of Advanced Technologies and Materials, Department of Physical Chemistry, Faculty of Science, Palacky University, 17. listopadu 12, 77146 Olomouc, Czech Republic

<sup>2</sup> Center for Superfunctional Materials, Department of Chemistry and Department of Physics, Pohang University of Science and Technology, Hyojadong, Namgu, Pohang 790-784, Korea

<sup>3</sup> Samsung Advanced Institute of Technology, 130 Samsung-ro, Yeongtong-gu, Suwon-si, Gyeonggi-do, 443-803, Korea

<sup>4</sup> Center for Superfunctional Materials, Department of Chemistry, Ulsan National Institute of Science and Technology (UNIST), UNIST-gil 50, Ulsan 689-798, Korea

E-mail: [petr.jurecka@upol.cz](mailto:petr.jurecka@upol.cz)

### Abstract

Hydrogen storage in carbonaceous materials and their derivatives is currently a widely investigated topic. Rational design of novel adsorptive materials is often attempted with the help of computational chemistry tools, in particular density functional theory (DFT). However, different exchange-correlation functionals provide a very wide range of hydrogen binding energies. The aim of this article is to offer high level QM reference data based on coupled-cluster singles and doubles calculations with perturbative triple excitations, CCSD(T), and a complete basis set limit estimate that can be used to assess the accuracy of various DFT-based predictions. For one complex, the CCSD(T) result is verified against diffusion quantum Monte Carlo calculation. Reference binding curves are calculated for two model compounds representing weak and strong hydrogen adsorption: coronene (-4.7 kJ/mol per H<sub>2</sub>), and coronene modified with boron and lithium (-14.3 kJ/mol). The reference data are compared to results obtained with widely used density functionals including pure DFT, M06, DFT-D3, PBE-TS, PBE+MBD, optB88-vdW, vdW-DF, vdW-DF2 and VV10. We find that whereas DFT-D3 shows excellent results for weak hydrogen adsorption on coronene, most of the less empirical density based dispersion functionals except VV10 overestimate this interaction. On the other hand, some of the less empirical density based dispersion functionals better describe stronger binding in the more polar corob<sub>2</sub>Li<sub>2</sub> ... 2H<sub>2</sub> complex which is one of realistic models for high-capacity hydrogen storage materials. Our results may serve as a guide for choosing suitable DFT methods for quickly evaluating hydrogen binding potential and as a reference for assessing the accuracy of the previously published DFT results.

## 1. Introduction

Recent progress in graphene-related nanotechnologies has fuelled interest in graphene-based sorption materials. One potential application of graphene nanostructures is in hydrogen storage devices. To be practical, these devices should match or exceed the target gravimetric capacity specified by the U.S. Department of Energy (DOE). In addition, they should adsorb molecular hydrogen reversibly. In the case of physisorption, the adsorption energy of molecular hydrogen should ideally be around 15 kJ/mol per H<sub>2</sub> in order to achieve the target capacity while still being weak enough to allow hydrogen release under relatively mild conditions.<sup>1</sup> Since the interaction energy of molecular hydrogen with a pristine graphene surface is only about 4 kJ/mol, several modifications of graphene have been proposed to increase the strength of this interaction.<sup>2-8</sup> While graphene surfaces can be doped with many elements, light elements such as boron, lithium, calcium or magnesium must be used to achieve the required gravimetric capacity.

In addition to experimental studies, there have been many attempts to use computational methods to design novel materials for hydrogen storage.<sup>5-12</sup> Typically, such studies use quantum mechanical (QM) methods to predict the geometries and properties of carbonaceous structures that incorporate light elements in order to enhance their interactions with molecular hydrogen.<sup>5-9,11,12</sup> A crucial quantity when designing graphene based sorption materials is the interaction energy, which can be related to the adsorption capacity of the studied material. Interaction energies are readily calculated using a wide variety of quantum chemical methods at various levels of accuracy and reliability.

The most popular tool for preliminary evaluation of hydrogen adsorption energy is density functional theory (DFT). This method is widely used due to its modest computational demands and ability to simulate reasonably large periodic structures. Unfortunately, the applicability of most current DFT functionals is limited by their inability to describe London dispersion forces. Because dispersion (long-range correlation) is an important part of the noncovalent binding energy to graphene-like materials, the reliability of results obtained with such DFT methods is often questionable. Note, however, that studies focusing on hydrogen chemisorption<sup>13,14</sup> are less sensitive to the quality of modeling of vdW interactions.

Considerable effort has been invested in the development of DFT methods that can describe dispersion interactions in recent years and many different solutions have been suggested.<sup>15-27</sup> Dispersion can be included either in the form of an empirical,<sup>15,17</sup> or with reduced empiricism at various levels of accuracy and computer demands.<sup>16,28-31</sup> Whereas some of these corrections have been extensively tested for various molecular systems,<sup>32-34</sup> their applications to hydrogen adsorption are still scanty.<sup>25,26</sup> For instance, an empirical DFT based DFT/CC scheme<sup>24</sup> with its parameters fitted to coupled cluster calculations (hence CC) described the interactions between molecular hydrogen and carbon nanostructures very accurately.<sup>25</sup> Therefore, it would be desirable to have a suitable benchmark for adsorptive hydrogen binding that would enable us to meaningfully compare different methods.

Accurate wave function theory QM methods can provide robust and reliable estimates of noncovalent binding.<sup>35-37</sup> However, very high levels of theory and considerable computer resources are needed to accurately describe weak dispersion interactions. Note that the popular and relatively affordable MP2 method is known to overestimate the dispersion contribution to the interaction energy<sup>38</sup> and thus is not suitable for benchmark calculations. Very accurate results can be obtained with the CCSD(T) method,<sup>39</sup> but only when large atomic basis sets are employed.<sup>40</sup> This makes calculations extremely demanding owing to the steep scaling of CCSD(T) demands ( $\approx O(N^7)$ ). One viable compromise is to estimate the CCSD(T) result at the complete basis set (CBS) limit by combining MP2/CBS extrapolation with corrections for higher-order correlation effects calculated using a smaller basis set,<sup>41</sup> and

also other possibilities exist.<sup>40</sup> However, studies of this type are limited to relatively small model systems, typically polyaromatic molecules, and are not suitable for production calculations.

Quantum Monte Carlo (QMC) calculations provide an alternative and largely independent source of theoretical reference data on interaction energies. The well-established diffusion Monte Carlo method with fixed node approximation<sup>42,43</sup> (FN-DMC) covers essentially all dynamic correlations and is thus (in this particular respect) equivalent to a full configuration interaction calculation using a complete basis set. FN-DMC calculations have successfully been used to study the interactions of atomic hydrogen (both chemi- and physisorption) with coronene and graphene.<sup>44</sup> While FN-DMC calculations are extremely time-consuming when very high accuracy (below 1 kJ/mol) is required,<sup>45</sup> they can provide invaluable help in situations where the accuracy of wave function based methods is not well established.<sup>46,47</sup>

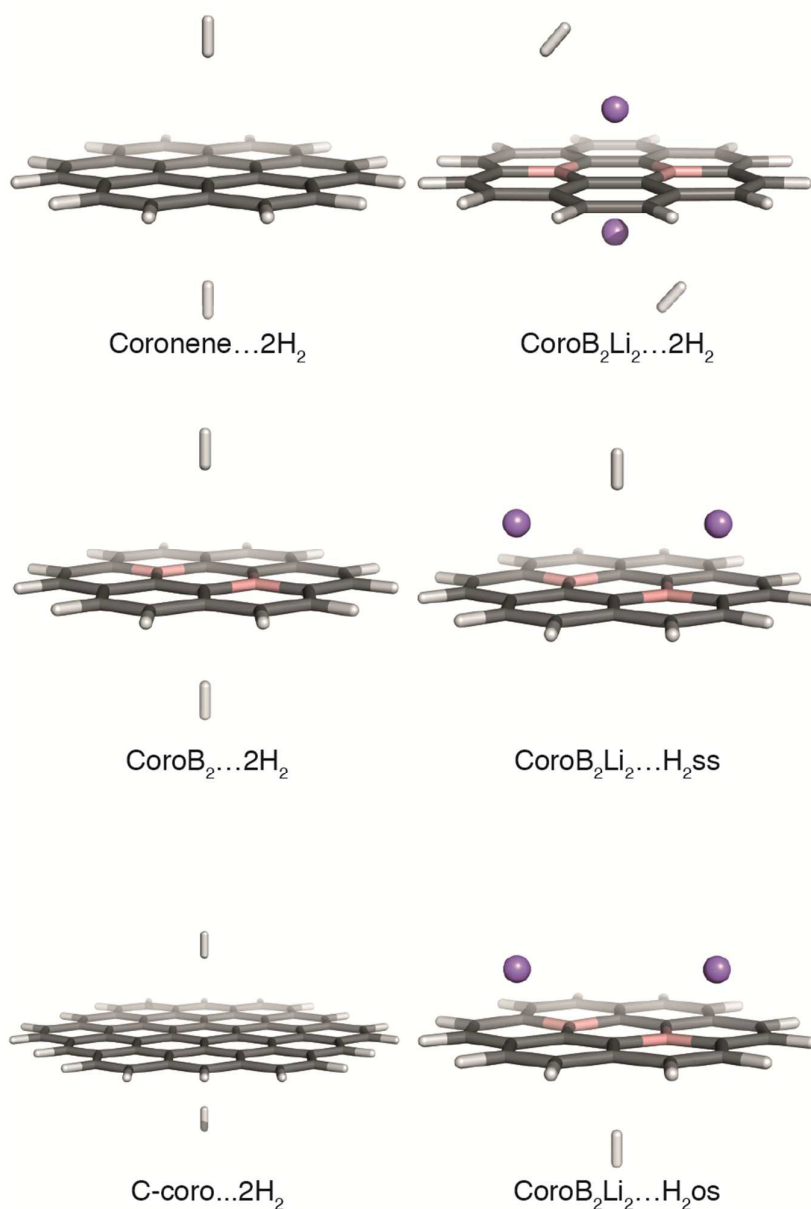
In this work we calculated reference dissociation curves for the physisorption of molecular hydrogen on two different model compounds, coronene and coronene modified with boron and lithium (coroB<sub>2</sub>Li<sub>2</sub>, Figure 1). Whereas coronene exhibits the weak hydrogen adsorption typical of unmodified carbonaceous materials, the coroB<sub>2</sub>Li<sub>2</sub> molecule exhibits much stronger molecular hydrogen binding characteristic of modified sorption materials. In addition, reference interaction energies were obtained for four additional model structures. Reference data were obtained using the high-level CCSD(T)/CBS method and FN-DMC calculations were performed to verify the wave function results for one complex. These reference results were then used to evaluate the performance of several standard DFT functionals along with some more recently developed DFT-based methods that include dispersion corrections.

## 2. Methods

**Structures.** Figure 1 shows small molecular complexes derived from coronene and circumcoronene which were chosen as models for graphene based materials. CoroB<sub>2</sub>Li<sub>2</sub>...2H<sub>2</sub> complex was designed as a model for strong adsorptive binding. Two atoms of coronene are replaced with boron atoms, which keep two attached lithium atoms in place. Hydrogen adsorbs on lithium atoms, due to its high affinity to this metal. Figure 1 shows also our largest model, which is circumcoronene...2H<sub>2</sub> complex (abbreviated as c-coro...2H<sub>2</sub>) and three additional complexes derived from coroB<sub>2</sub>Li<sub>2</sub> by moving and replacing lithium atoms: coroB<sub>2</sub>Li<sub>2</sub>ss...2H<sub>2</sub> with lithium atoms placed on the same side of coronene skeleton and one hydrogen molecule bound from the other side (weak binding), coroB<sub>2</sub>Li<sub>2</sub>os...2H<sub>2</sub> with lithium atoms placed on the same side and one hydrogen molecule bound directly to them (strong binding) and finally coroB<sub>2</sub>...2H<sub>2</sub> with one hydrogen molecule bound on each side (weak bonding). All structures were optimized using the TPSS functional augmented with an empirical dispersion term using the B-0.93-35 parameters<sup>17</sup> and the cc-pVQZ basis set. During this optimization, the distance between the hydrogen atoms of molecular hydrogen was held at its CCSD(T)/AVQZ-optimized value (0.742 Å).<sup>25</sup> Symmetric structures with two H<sub>2</sub> molecules placed above and below the coronene base (Figures 1 and 2) were used to reduce the demands of the time-consuming CCSD(T) calculations by exploiting symmetry. The error due to the presence of the second H<sub>2</sub> molecule was found to be smaller than 0.05 kJ/mol at the MP2/CBS level and approximately similar on the DFT PBE/aug-cc-pVQZ level. Starting from the resulting optimized structures, geometries for a distance-dependent scan were generated by varying only the intermolecular separation between the sorbent and hydrogen molecules (2.5, 2.8, 3.1, 3.4, 3.7, 4.0, 5.0 and 7.0 Å). Interaction energies were calculated as the difference in energy between the complex and the isolated coronene as one

subsystem and two isolated hydrogen molecules as the second. All interaction energies are given per one H<sub>2</sub> molecule.

**Figure 1.** Model complexes.



**Reference CCSD(T)/CBS Calculations.** Reference QM interaction energies were calculated according to Eq. 1.

$$\Delta E_{\text{CBS}}^{\text{CCSD(T)}} = \Delta E_{\text{CBS}}^{\text{MP2}} + (\Delta E^{\text{CCSD(T)}} - \Delta E^{\text{MP2}})_{\text{small basis}} \quad \text{Eq. 1}$$

The MP2 energy at the complete basis set (CBS) limit ( $\Delta E_{\text{CBS}}^{\text{MP2}}$ ) was obtained using the 2-point extrapolation scheme of Halkier and Helgaker, in which HF and correlation energies are extrapolated separately.<sup>48,49</sup> For these calculations, the hydrogen molecules and the inner ring atoms of coronene (6 carbon atoms) and coroB<sub>2</sub>Li<sub>2</sub> (4 carbon, 2 boron, and 2 lithium

atoms) were described using the aug-cc-pVXZ basis sets (X=T,Q), while the remaining carbon and hydrogen atoms were described using the cc-pVXZ (X=T,Q) basis sets and analogically for corob<sub>2</sub>Li<sub>2</sub>, corob<sub>2</sub>Li<sub>2</sub>ss, corob<sub>2</sub>Li<sub>2</sub>os and circumcoronene complexes.

The correction for higher order correlation effects ( $\Delta E^{\text{CCSD(T)}} - \Delta E^{\text{MP2}}$ ) was calculated as the difference between the CCSD(T) and MP2 energies obtained using a smaller basis set. The use of a smaller basis set is justified by the weak basis set dependence of this contribution.<sup>50</sup> For the complexes derived from coronene we used the QZVPP basis set for the H<sub>2</sub> molecules, the TZVPP basis set for the inner ring atoms and lithium and the TZVP basis set for the remaining atoms. The  $\Delta E^{\text{CCSD(T)}} - \Delta E^{\text{MP2}}$  correction obtained with this basis set was found to be very close (difference less than 0.03 kJ/mol) to the correction obtained with larger aug-cc-pVTZ basis set on inner ring atoms and molecular hydrogen for the optimal geometry of coronene...H<sub>2</sub> complex. For more details on basis set dependence of  $\Delta E^{\text{CCSD(T)}} - \Delta E^{\text{MP2}}$  correction see e.g. ref.<sup>51</sup>. In case of circumcoronene we used TZVP basis for hydrogen molecules, SVP basis for the inner ring atoms and SV basis for the remaining circumcoronene atoms. Counterpoise correction was used in all calculations. The CCSD(T)/CBS evaluation is described in more detail elsewhere.<sup>41</sup> CCSD(T) and MP2 calculations were performed using the TurboMole 6.3 software package.<sup>52,53</sup>

**Reference Quantum Monte Carlo Calculations.** Benchmark diffusion quantum Monte Carlo ground-state projection calculations<sup>45</sup> for the coronene...H<sub>2</sub> complex were performed in qWalk code<sup>54</sup> using the single-determinant Slater-Jastrow trial wave functions, which are known to provide an optimal cost/accuracy tradeoff (cf. e.g. ref.<sup>55,56</sup>). B3LYP orbitals used in determinants were calculated in GAMESS code<sup>57</sup> with the aug-cc-pVTZ basis set and the core electrons were replaced by the appropriate effective core potentials.<sup>58</sup> The explicit correlation Jastrow terms containing electron-nucleus (e-n) and electron-electron (e-e) contributions were expanded in polynomial Padé functions and their variational parameters were fully optimized within variational Monte Carlo separately for the complex and its constituents.<sup>59</sup> The employed protocol<sup>60</sup> exhibits favorable scaling,  $\propto O(N^3)$  where  $N$  is the number of electrons, and relies on fixed-node error cancellation.<sup>45</sup> It has been shown to be suitable for benchmark calculations of noncovalent interaction energies in larger closed-shell complexes.<sup>59,61</sup> The statistical error is reported as  $\pm$  the standard deviation ( $\sigma$ ).

**SAPT Decomposition of Interaction Energies.** The components of the interaction energy between the sorbent and H<sub>2</sub> molecules were determined by the DFT-SAPT method of Hesselmann and Jansen<sup>62-65</sup> as implemented in the Molpro software package.<sup>66</sup> In DFT-SAPT, the monomer is described using density functional theory (DFT) and the intermolecular interactions by SAPT (Symmetry Adapted Perturbation Theory).<sup>67</sup> The total interaction energy is then given by the sum of the following terms (Eq. 2)

$$E^{\text{SAPT}} = E_{\text{elst}}^{(1)} + E_{\text{exch}}^{(1)} + E_{\text{ind}}^{(2)} + E_{\text{exch-ind}}^{(2)} + E_{\text{disp}}^{(2)} + E_{\text{exch-disp}}^{(2)} + \delta(\text{HF}), \quad (\text{Eq. 2})$$

where  $E_{\text{elst}}^{(1)}$  is the electrostatic contribution,  $E_{\text{exch}}^{(1)}$  is the exchange repulsion contribution,  $E_{\text{ind}}^{(2)}$  is the induction or polarization contribution,  $E_{\text{disp}}^{(2)}$  is the dispersion contribution, and  $E_{\text{exch-ind}}^{(2)}$  and  $E_{\text{exch-disp}}^{(2)}$  are exchange-induction and exchange-dispersion mixing terms. The  $\delta(\text{HF})$  term approximates higher order induction contributions. Here, these contributions are conveniently contracted into four terms:  $E_{\text{elst}} = E_{\text{elst}}^{(1)}$ ,  $E_{\text{exch}} = E_{\text{exch}}^{(1)}$ ,  $E_{\text{ind}} = E_{\text{ind}}^{(2)} + E_{\text{exch-ind}}^{(2)} + \delta(\text{HF})$  and  $E_{\text{disp}} = E_{\text{disp}}^{(2)} + E_{\text{exch-disp}}^{(2)}$ . All DFT-SAPT calculations were done using the cc-pVTZ basis set and PBE0AC density functional<sup>63,68,69</sup> with the asymptotically correct LB94 xc-potential of van Leeuwen and Baerends<sup>70</sup> and a gradient-controlled shift procedure.<sup>71</sup>

**DFT calculations.** Some of the most commonly used density functionals were evaluated: the LDA SVWN functional,<sup>72,73</sup> the GGA functionals BLYP,<sup>74,75</sup> PBE,<sup>68</sup> B97-D<sup>76</sup> and PW91,<sup>77</sup> the hybrid functionals B3LYP<sup>78</sup> and PBE0,<sup>69</sup> and the meta-GGA functional TPSS<sup>79</sup> and hybrid meta-GGA functional M06.<sup>80</sup> These DFT calculations were performed using the def2-QZVP basis set and some were also performed using the def2-TZVP basis set for comparative purposes. Calculations using Grimme's semi-classical dispersion correction (DFT-D3) were performed with the basis set recommended by the authors (def2-QZVP) in conjunction with Johnson and Becke damping,<sup>20,81,82</sup> both with and without damped Axilrod-Teller-Muto (ATM) based three-body terms.<sup>16</sup> Counterpoise correction was not applied. DFT calculations were carried out in TurboMole 6.3 software,<sup>52</sup> except for M06 and PW91 calculations which were performed in Gaussian 09 core.<sup>83</sup> Calculations with the Tkatchenko-Scheffler PBE-TS<sup>21</sup> and PBE+MBD many-body dispersion (MBD correction on top of self consistent screening, SCS)<sup>29</sup> methods were performed using the FHI-aims code<sup>84</sup> with a tier 2 basis set and a tight grid (note that a revised MBD@rsSCS method has recently been introduced, which is, however, not tested here.)<sup>30,46</sup> VV10<sup>28</sup> calculations were performed in Q-Chem code<sup>85</sup> with cc-pVTZ basis set, except for circumcoronene complex which was described by cc-pVDZ basis set. The VASP code<sup>86</sup> was used to calculate vdW-DF,<sup>18</sup> vdW-DF2<sup>87</sup> and optB88-vdW<sup>88</sup> interaction energies in a 20x20x25 Å rectangular box with a 500 eV cutoff.

### 3. Results and Discussion

**Nature of Binding in Model Complexes.** Knowing the nature of hydrogen's interactions with different types of sorbents may help us to understand the performance of various density functional based methods. It has been shown that dispersion interactions dominate the binding of both polar and non-polar solvent molecules to coronene,<sup>89,90</sup> and may also be important in hydrogen storage materials.<sup>91</sup> Because H<sub>2</sub> is a nonpolar molecule we would expect dispersion forces to similarly dominate the stabilizing interaction in the coronene...2H<sub>2</sub> complex. However, in the corob<sub>2</sub>Li<sub>2</sub> complex hydrogen binds to partially cationic lithium atoms. As such, the polarization contribution may also be important in this case. To assess the relative importance of these stabilizing contributions, we decomposed the total interaction energy of the two above mentioned complexes into physically meaningful contributions using the DFT-SAPT method. The interaction energy can be decomposed into four basic components: electrostatic, induction (or polarization), dispersion and repulsion.

Table 1 shows that dispersion is, as expected, by far the most important contribution in the coronene...2H<sub>2</sub> complex, accounting for about 75% of its total stabilization. The second largest contribution (18%) is from electrostatic stabilization. This comes in part from the overlap (penetration) effect and in part from the interaction of coronene's molecular quadrupole with that of the H<sub>2</sub> molecule. Note that while the quadrupolar component is important for small model compounds such as benzene or coronene, it will be close to zero for infinite planar graphene sheets due to the cancellation of the quadrupolar field in this case. For this reason the coronene molecule may not be a fully representative model for interactions with infinite graphene. However, it should also be noted that quadrupolar interactions may become sizeable even in graphene, either on the edges of finite graphene flakes or when the graphene is corrugated as is often the case.<sup>92</sup>

The situation with the corob<sub>2</sub>Li<sub>2</sub> complex is different. While the dispersion contribution is still quite large in this case, the polarization and electrostatic contributions are equally important; their combined stabilizing contribution is about twice that of dispersion. Because of its additional induction and electrostatic stabilization, this complex is much more stable than coronene...2H<sub>2</sub>.

**Table 1.** Components of the interaction energy (kJ/mol per H<sub>2</sub>) in model complexes obtained using SAPT decomposition at the equilibrium geometry.

Complex	E <sub>Exch-rep</sub>	E <sub>EIst</sub>	E <sub>Ind</sub>	E <sub>Disp</sub>	E <sub>Tot</sub>
coronene...2H <sub>2</sub>	6.5	-1.8	-0.8	-7.4	-3.5
coroB <sub>2</sub> Li <sub>2</sub> ...2H <sub>2</sub>	22.0	-13.0	-12.1	-10.9	-14.0

The calculations described above show that the nature of hydrogen binding in nonpolar and polar complexes is very different. This should be reflected in the performance of DFT functionals for the two binding situations. As we show below, DFT methods without explicit dispersion correction perform poorly for the dispersion-dominated (weakly bound) complexes but their results for the dispersion/induction-stabilized (strongly bound) complexes are in much better (albeit imperfect) agreement with reference calculations.

**Reference CCSD(T)/CBS and FN-DMC calculations.** The reference dissociation curves obtained at the CCSD(T)/CBS level are shown in Figure 2. For the coronene...2H<sub>2</sub> complex, our calculations predict an interaction energy of -4.68 kJ/mol per H<sub>2</sub> molecule. This result is comparable to other CCSD(T)/CBS estimates that have been published for smaller model systems. As expected, the calculated binding energy for coronene is greater than that reported for benzene (-4.34 kJ/mol) or naphthalene (-4.42 kJ/mol).<sup>25</sup> Our reference value is also in relatively good agreement with the partly empirical DFT/CC estimate for coronene obtained by the same authors (-4.94 kJ/mol), particularly given that the DFT/CC potential was found to overestimate the interaction energy of hydrogen with graphene by 0.2 kJ/mol.<sup>93</sup>

The reliability of the CCSD(T)/CBS estimate was confirmed by a single point FN-DMC calculation on the coronene...H<sub>2</sub> complex at the equilibrium separation (3.1 Å). The FN-DMC run provided an interaction energy of  $-4.31 \pm 0.7$  kJ/mol, in good agreement with the wave function result. Note that the CCSD(T)/CBS and FN-DMC methods are quite different in nature but are both regarded as benchmark-quality approaches. As such, this good agreement gives us confidence in the accuracy of our result.

The largest model system for which we were able to perform CCSD(T)/CBS calculations was circumcoronene...2H<sub>2</sub> with interaction energy -5.55 kJ/mol per hydrogen molecule. This value is somewhat larger than we would expect for an intermediate between coronene and graphene (see below). However, we should note that relatively small basis set was used to evaluate ( $\Delta E^{\text{CCSD(T)}} - \Delta E^{\text{MP2}}$ ) correction in this complex (see Methods). In our experience, smaller basis sets provide smaller (positive) ( $\Delta E^{\text{CCSD(T)}} - \Delta E^{\text{MP2}}$ ) correction, which might explain overestimation of interaction strength in this complex. Therefore, we will base further discussion on coronene based complexes, for which relatively large basis sets were used.

Comparison of our theoretical estimates with experimental data is not straightforward. First, experimental data are available only for the interaction of molecular hydrogen with graphite ( $-51.7 \pm 0.5$  meV, or  $-4.99 \pm 0.05$  kJ/mol);<sup>94</sup> its interaction with graphene is expected to be around 9 % weaker,<sup>95</sup> i.e., ca -4.44 kJ/mol. Second, the interaction of H<sub>2</sub> with graphene is expected to be stronger than with our model molecule, coronene; the difference between the two is estimated to be -0.5 kJ/mol based on DFT/CC calculations<sup>25</sup> giving interaction energy with graphene -5.18 kJ/mol. This indicates that our CCSD(T)/CBS calculations may somewhat overestimate interaction energy. However, we would like to note that both above mentioned corrections (graphite-to-graphene and coronene-to-graphene) are only approximate estimates and in case of graphite-to-graphene correction smaller values were reported in literature.<sup>96</sup>

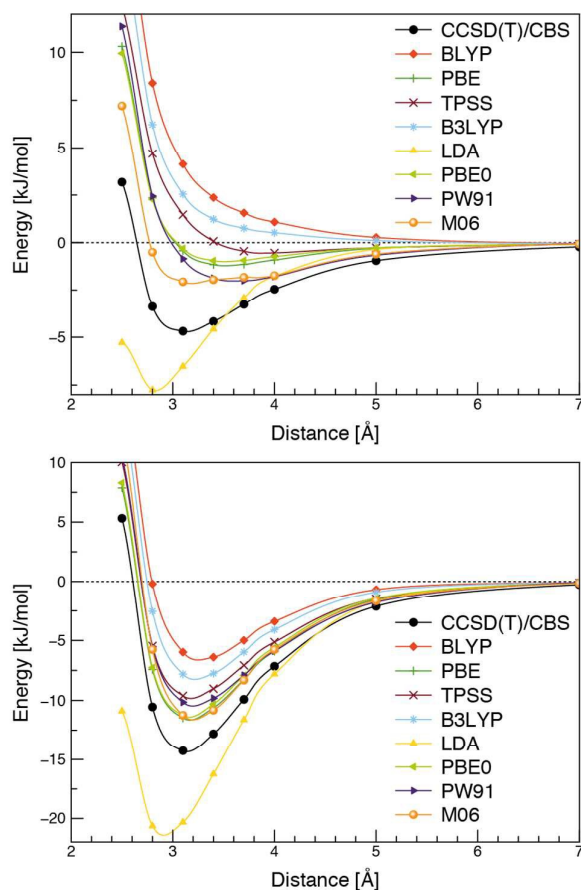
Reference interaction curves for the more polar corob<sub>2</sub>Li<sub>2</sub>...2H<sub>2</sub> complex are also shown in Figure 2. The accuracy of these results should be similar to those for the complex of

coronene with molecular hydrogen. The estimated interaction energy is -14.25 kJ/mol per H<sub>2</sub> molecule. Note that this large interaction energy is close to the optimal value suggested by Bhathia et al.<sup>1</sup> (15 kJ/mol), so the coronene...2H<sub>2</sub> complex should be a good model system for studying adsorptive hydrogen storage.

**Pure DFT Functionals.** Let us start with the dispersion-bound complex of molecular hydrogen with coronene. Given the importance of dispersion in this complex, it can be expected that the widely used LDA, GGA, meta-GGA and hybrid density functionals will not describe it correctly. Indeed, as shown in Figure 2 all GGA based functionals with the def2-QZVP atomic basis set either predict that hydrogen does not bind (BLYP, B3LYP) or underestimate its binding to varying extents, depending on the level of error cancellation in their exchange-correlation parts. Similar results were obtained with the smaller def2-TZVP basis set (not shown). In addition, the equilibrium binding distances predicted by these functionals are too long. The M06 hybrid meta-GGA functional developed by Truhlar's group yields the best agreement with the reference curve and also predicts the right intermolecular distance. However, even M06 underestimates binding quite significantly, by more than 50%. Thus, none of the pure (dispersion uncorrected) functionals can be recommended for the investigation of weak H<sub>2</sub> binding to nonpolar carbonaceous sorbents.

The SVWN LDA functional is also unsuitable for describing hydrogen adsorption on nonpolar adsorbents. According to Figure 2, it overestimates the binding energy in the coronene...2H<sub>2</sub> complex by about 50% and also predicts too short an equilibrium distance. Strong overestimation of binding by SVWN has been reported previously, and its source has been traced to the erroneous exchange functional.<sup>97</sup> Therefore, predicted sorption energies on novel materials obtained with this functional will probably be unrealistically large.

**Figure 2.** DFT/def2-QZVP interaction energies compared to CCSD(T)/CBS reference data for the coronene...2H<sub>2</sub> (top) and corob<sub>2</sub>Li<sub>2</sub>...2H<sub>2</sub> (bottom) complexes. Interaction energies are given per one H<sub>2</sub> molecule.



Next, we compare the performance of different functionals for the corob<sub>2</sub>Li<sub>2</sub>...2H<sub>2</sub> complex, in which molecular hydrogen is bound much more strongly than in the coronene complex (-14.3 kJ/mol vs. -4.7 kJ/mol). As shown above, this is largely due to additional stabilization arising from electrostatics and polarization. Because standard DFT functionals describe polarization-bound complexes relatively well (although some error cancellation is involved),<sup>98</sup> we would expect them to perform comparatively well for this complex. Indeed, Figure 2 shows that in this case all tested functionals predict bonding and none of them is purely repulsive. The best agreement is achieved with the M06, PBE and PBE0 functionals, which underestimate the interaction energy by about 20% relative to the reference CCSD(T)/CBS data (see Table 2) and predict the correct intermolecular separation. The PW91 and TPSS functionals also predict relatively accurate binding distances but substantially underestimate the interaction energy. The other functionals predict only weak binding, giving less than half of the reference interaction energy. As before, the SVWN functional strongly overestimates the interaction energy. Results for the remaining tested structures are similar (Table 2).

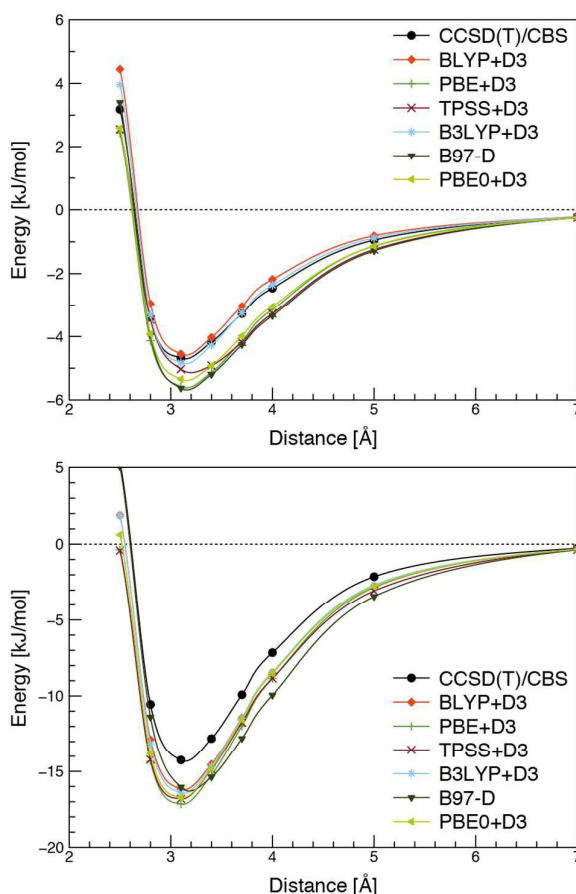
**Table 2.** Interaction energies per one H<sub>2</sub> molecule (kJ/mol) calculated for equilibrium separations obtained at CCSD(T)/CBS level for the coronene...2H<sub>2</sub> and coroB<sub>2</sub>Li<sub>2</sub>...2H<sub>2</sub> complexes and on the TPSS/B-0.93-35 level for the remaining complexes. D3 stands for dispersion correction and ATM for Axilrod-Teller-Muto three-body correction. \*VV10 interaction energy for c-coro...2H<sub>2</sub> complex was obtained with a smaller cc-pVDZ basis set.

Method	coronene...2H <sub>2</sub>			coroB <sub>2</sub> Li <sub>2</sub> ...2H <sub>2</sub>			coroB <sub>2</sub> ...2H <sub>2</sub>			coroB <sub>2</sub> Li <sub>2</sub> ...H <sub>2</sub> ss			coroB <sub>2</sub> Li <sub>2</sub> ...H <sub>2</sub> os			c-coro...2H <sub>2</sub>		
	ΔE	+D3	+ATM	ΔE	+D3	+ATM	ΔE	+D3	+ATM	ΔE	+D3	+ATM	ΔE	+D3	+ATM	ΔE	+D3	+ATM
<b>CCSD(T)/CBS</b>	<b>-4.7</b>			<b>-14.3</b>			<b>-4.9</b>			<b>-10.4</b>			<b>-5.0</b>			<b>-5.5</b>		
BLYP	4.1	-4.5	-4.2	-6.0	-16.2	-15.9	4.1	-4.5	-4.2	-0.2	-13.2	-12.9	3.2	-4.5	-4.3	4.1	-5.0	-4.6
PBE	-0.4	-5.6	-5.3	-11.5	-17.2	-16.9	-0.7	-5.8	-5.5	-7.2	-14.2	-13.9	-1.4	-6.0	-5.7	-0.4	-5.9	-5.5
TPSS	1.5	-5.0	-4.7	-9.6	-16.8	-16.5	1.2	-5.2	-4.9	-4.8	-13.8	-13.5	0.5	-5.4	-5.1	1.5	-5.4	-5.0
B3LYP	2.5	-4.8	-4.5	-7.8	-16.4	-16.1	2.5	-4.8	-4.5	-2.1	-13.0	-12.7	1.8	-4.8	-4.5	2.5	-5.3	-4.9
PBE0	-0.3	-5.3	-5.0	-11.3	-16.7	-16.4	-0.6	-5.6	-5.2	-6.9	-13.6	-13.3	-1.1	-5.7	-5.4	-0.4	-5.8	-5.4
B97D	-5.6			-16.0			-5.7			-14.9			-5.7			-6.0		
LDA	-6.5			-20.3			-7.1			-17.3			-7.1			-6.6		
PW91	-0.8			-10.2			-0.5			-8.6			-2.4			-1.6		
M06	-2.1			-11.2			-2.4			-12.5			-4.2			-3.5		
PBE+TS	-6.0			-16.1			-5.0			-15.7			-7.0			-6.5		
PBE+MBD	-5.3			-22.8			-4.3			-22.8			-5.8			-5.7		
optB88+vdW	-5.9			-15.2			-4.7			-12.1			-6.5			-6.7		
vdW-DF	-6.6			-14.5			-4.5			-9.7			-6.4			-6.7		
vdW-DF2	-5.5			-15.1			-4.1			-10.5			-6.0			-6.1		
VV10	-5.1			-16.0			-3.9			-12.9			-5.8			-4.7*		

These results clearly show that none of the tested DFT functionals is capable of accurately describing hydrogen physisorption in both dispersion and polar binding scenarios. The best results are obtained with M06, but even this functional substantially underestimates the strength of binding in both complexes. The other DFT functionals, which have often been used to estimate adsorption strength in the literature, predict excessively weak binding. The only exception is SVWN, which strongly overestimates the interaction energy. Thus, none of the standard and widely used DFT functionals can be used to accurately estimate hydrogen adsorption on carbonaceous materials.

**Functionals with Semi-Classical Dispersion Correction.** The semi-classical dispersion corrections start from the classical atom-atom pairwise scheme. The DFT-D3 method developed by Grimme was tested because it is widely available and can be combined with various commonly used DFT functionals. In addition we tested also B97-D functional and PBE-TS and PBE+MBD functionals of Tkatchenko and Scheffler. Whereas DFT-D3, PBE-TS and PBE+MBD methods involve some kind of coordination number (D3) or density based (TS and MBD) adjustment of input parameters, older B97D scheme is more empirical. Figures 3 and 4 and Table 2 show the results obtained with these density functionals. As expected, the dispersion correction improved the overall accuracy of the DFT predictions for both the dispersion-bound and the polar complexes. All functionals predicted equilibrium geometries very close to the CCSD(T)/CBS reference (Figures 3 and 4). For the complexes in which hydrogen molecule is not in contact with lithium atoms, especially DFT-D3 methods provided fairly accurate results. The PBE+TS method overestimated interaction strength in some complexes, but this was largely corrected by many-body dispersion correction. Interestingly, most of the tested functionals somewhat overestimated the interaction energy in the complexes with molecular hydrogen bound to lithium. Note that PBE+MBD method predicted much too strong binding (results are not shown in Figure 4 but single point calculations are reported in Table 2). Because similar strong overestimation was observed for both complexes in which lithium was in contact with hydrogen molecule (see Table 2), we suspect that the problem may be specific for this particular situation (partially cationic lithium) as PBE+MBD was shown to perform very well for a wide variety of molecular complexes.<sup>23,33</sup> Thus, the semi-classical dispersion corrections provided clear improvements, although some of the methods tend to overestimate interaction strength.

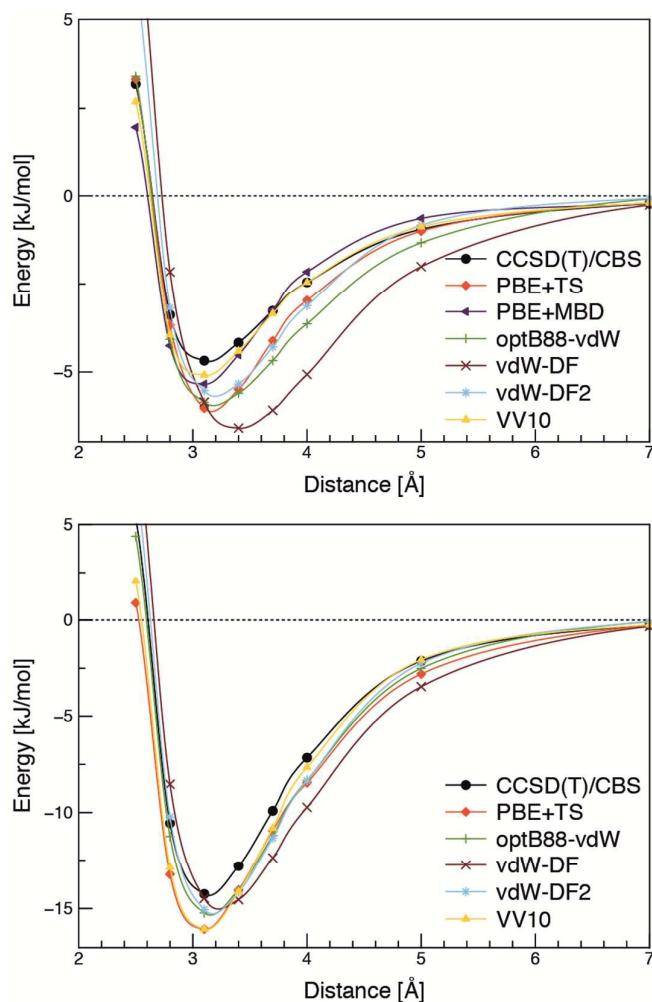
**Figure 3.** DFT-D3 and B97-D interaction energies (def2-QZVP basis set) compared to CCSD(T)/CBS reference data for the coronene...2H<sub>2</sub> (top) and coroB<sub>2</sub>Li<sub>2</sub>...2H<sub>2</sub> (bottom) complexes. Interaction energies are given per one H<sub>2</sub> molecule.



**Importance of the Three-Body Dispersion Term.** Optionally, DFT-D3 calculations can be performed using an empirical correction for three-body dispersion based on the Axilrod-Teller-Muto formula (see above). Interaction energies with ATM correction calculated for a separation of 3.1 Å (equilibrium geometry) for selected DFT-D3 combinations are shown in Table 2. Inclusion of the three-body terms slightly weakens the predicted interaction regardless of the DFT-D3 functional used. Thus, three body terms somewhat improved the agreement between the DFT-D3 functionals and the reference calculations when the DFT-D3 calculations were too attractive and vice versa. However, this effect was very modest, amounting to around 0.3 kJ/mol on average (note that the non-additivity of dispersion can become large in larger complexes.<sup>23,99,100</sup> It therefore seems that inclusion of the three-body dispersion correction is less critical, but selection of an accurate combination of DFT functional and two-body D3 correction is important.

**Functionals with Density-Based Dispersion Correction.** Several density functionals in which the dispersion correction is largely derived from the DFT electron density are now available in widely used quantum chemistry packages. Here we tested the vdW-DF functional of Dion et al.,<sup>18</sup> its newer version vdW-DF2,<sup>87</sup> a reparameterization of vdW-DF developed by Klimes et al.<sup>88</sup> (optB88-vdW) and the VV10 functional.<sup>28</sup> Results are shown in Figure 4 and Table 2.

**Figure 4.** PBE+TS, vdW-DF, vdW-DF2 and optB88-vdW interaction energies compared to CCSD(T)/CBS reference data for the coronene...2H<sub>2</sub> (top) and corob<sub>2</sub>Li<sub>2</sub>...2H<sub>2</sub> (bottom) complexes. Interaction energies are given per one H<sub>2</sub> molecule.



All vdW-DF based functionals overestimated the binding energy in the nonpolar coronene...2H<sub>2</sub> complex (Figure 4), except for PBE+MBD, which slightly underestimated binding above 4 Å. The largest discrepancy was seen for vdW-DF, which also overestimated the equilibrium separation by about 30%. The newer vdW-DF2 and optB88+vdW functionals performed better and predicted correct equilibrium separation. Similar results were obtained also for the weakly bound corob<sub>2</sub>Li<sub>2</sub>...H<sub>2</sub>os and c-coro...2H<sub>2</sub> complexes, however, not for the corob<sub>2</sub>...2H<sub>2</sub> complex (Table 2). VV10 functional predicted smallest stabilization energies for weakly bound cases and is in the best agreement with the CCSD(T)/CBS reference for coronene...2H<sub>2</sub> complex. In the strongly bound complexes with lithium in contact with hydrogen all density-based dispersion functionals overestimated the interaction energy to varying extent. In contrast to the dispersion bound complexes described above the VV10 functional predicted the largest overestabilization here. Nevertheless, in spite of the tendency to overestimation of interaction energy it is clear that inclusion of dispersion energy represents an improvement compared to pure DFT functionals.

Finally, we would like to note that in addition to the system dependence described above, performance of the tested methods may also be size dependent. We did not consider large molecular models in this work because our aim was to provide comparison of DFT based methods for model molecules for which accurate CCSD(T)/CBS estimate was possible. For scaling properties as a function of system size we refer the reader to other works concerning larger polyaromatic hydrocarbons<sup>96</sup> or their interaction with small molecules.<sup>25,51</sup>

#### 4. Conclusions

The accuracy of various DFT based approaches for estimating the adsorption energies of molecular hydrogen to two model compounds was assessed by comparison to high-level wave function theory and Diffusion Quantum Monte Carlo reference calculations. Two binding scenarios were considered: weak dispersion-dominated binding to a coronene, boron-doped coronene and circumcoronene and strong polar binding to lithium placed on boron-doped coronene models.

In the weak binding case, the common GGA, meta-GGA and hybrid functionals significantly underestimate the interaction energy and cannot be recommended for quantitative estimates. It is important to emphasize that the frequently used pure LDA functional strongly overbinds hydrogen and predicts excessively short intermolecular separations in both types of complexes. As such, its use is generally not recommended. Predictions based on LDA calculations would result in unrealistically favorable binding of molecular hydrogen. Various types of dispersion corrections to DFT, whether semi-classical or density based, generally improve the predicted binding energies and geometries, and several schemes provide very accurate results. In particular, computationally inexpensive DFT-D3 method provides fairly robust interaction energies and accurate optimal geometries. Among the tested density based dispersion correction schemes, the vdW-DF2, optB88+vdW and VV10 provided significantly better results than pure DFT functionals. Nevertheless, they somewhat overestimate the binding energy and their overall accuracy was lower than that of the best semi-classical DFT-D3 combinations.

The more polar  $\text{coroB}_2\text{Li}_2 \dots 2\text{H}_2$  complex is probably a better model for potential high capacity graphene-based sorbent materials. In this case, the DFT functionals without dispersion correction underestimate binding, although to a lesser extent than for the weak binding case. The best pure DFT functionals in this case are M06, PBE and PBE0, which underestimate the binding strength by less than 20 %. The inclusion of dispersion corrections increases the overall accuracy of the predictions also for the stronger bound complexes, although there is a notable tendency to overestimate interaction energies. The most accurate dispersion-corrected functionals were the density-based vdW-DF2 and optB88+vdW and also computationally inexpensive DFT-D3 methods performed well, providing also very accurate equilibrium geometries.

Our results may serve as a guide for choosing a suitable DFT method for quickly predicting the strength of hydrogen binding in new materials and as a reference for assessing the accuracy of previously published DFT results. Note, however, that the results should be generalized with caution, because performance of some of the tested methods may be system dependent. This is exemplified by very good accuracy of the semi-classical dispersion correction schemes for the weakly bound complexes that resemble binding situations considered in the method development, which is in contrast with the notable overestimation of interaction energy in complexes containing partially cationic lithium atoms.

**Acknowledgements.** The authors thank Vojtěch Krajňanský for help with designing the model complexes. This work was supported by grant P208/12/G016 from the Grant Agency of the Czech Republic (P.J., M.O.), by the Operational Program Research and Development for Innovations of the European Regional Development Fund (CZ.1.05/2.1.00/03.0058) and project No. CZ.1.07/2.3.00/20.0058, administered by the Ministry of Education, Youth and Sports of the Czech Republic. Further funding was provided by NRF (National Honor Scientist Program: 2010-0020414), the OP Education for Competitiveness - European Social Fund, project CZ.1.07/2.3.00/30.0004 (M.D.) and the Student Project IGA\_PrF\_2014023 of Palacky University".

## References

1. S. K. Bhatia and A. L. Myers, *Langmuir*, 2006, **22**, 1688–1700.
2. K. C. Kemp, H. Seema, M. Saleh, N. H. Le, K. Mahesh, V. Chandra, and K. S. Kim, *Nanoscale*, 2013, **5**, 3149–3171.
3. H. M. Lee, D. Y. Kim, C. Pak, N. J. Singh, and K. S. Kim, *J. Chem. Theory Comput.*, 2011, **7**, 969–978.
4. V. Georgakilas, M. Otyepka, A. B. Bourlinos, V. Chandra, N. Kim, K. C. Kemp, P. Hobza, R. Zbořil, and K. S. Kim, *Chem. Rev.*, 2012, **112**, 6156–6214.
5. Y.-H. Kim, Y. Zhao, A. Williamson, M. Heben, and S. Zhang, *Phys. Rev. Lett.*, 2006, **96**, 016102.
6. A. Du, Z. Zhu, and S. C. Smith, *J. Am. Chem. Soc.*, 2010, **132**, 2876–2877.
7. W.-Q. Deng, X. Xu, and W. Goddard, *Phys. Rev. Lett.*, 2004, **92**, 166103.
8. B. Kuchta, L. Firlej, S. Roszak, and P. Pfeifer, *Adsorption*, 2010, **16**, 413–421.
9. L. Firlej, S. Roszak, B. Kuchta, P. Pfeifer, and C. Wexler, *J. Chem. Phys.*, 2009, **131**, 164702.
10. S. Patchkovskii, J. S. Tse, S. N. Yurchenko, L. Zhechkov, T. Heine, and G. Seifert, *Proc. Natl. Acad. Sci. U. S. A.*, 2005, **102**, 10439–10444.
11. H. Lee, J. Ihm, M. L. Cohen, and S. G. Louie, *Nano Lett.*, 2010, **10**, 793–798.
12. I. Cabria, M. J. López, and J. A. Alonso, *J. Chem. Phys.*, 2005, **123**, 204721.
13. M. Bonfanti, R. Martinazzo, G. F. Tantardini, and A. Ponti, *J. Phys. Chem. C*, 2007, **111**, 5825–5829.
14. G. M. Psfogiannakis, T. a Steriotis, A. B. Bourlinos, E. P. Kouvelos, G. C. Charalambopoulou, A. K. Stubos, and G. E. Froudakis, *Nanoscale*, 2011, **3**, 933–936.

15. S. Grimme, *J. Comput. Chem.*, 2004, **25**, 1463–1473.
16. S. Grimme, J. Antony, S. Ehrlich, and H. Krieg, *J. Chem. Phys.*, 2010, **132**, 154104.
17. P. Jurečka, J. Černý, P. Hobza, and D. R. Salahub, *J. Comput. Chem.*, 2007, **28**, 555–569.
18. M. Dion, H. Rydberg, E. Schröder, D. C. Langreth, and B. I. Lundqvist, *Phys. Rev. Lett.*, 2004, **92**, 246401.
19. A. D. Becke and E. R. Johnson, *J. Chem. Phys.*, 2007, **127**, 154108.
20. E. R. Johnson and A. D. Becke, *J. Chem. Phys.*, 2005, **123**, 24101.
21. A. Tkatchenko and M. Scheffler, *Phys. Rev. Lett.*, 2009, **102**, 073005.
22. S. N. Steinmann and C. Corminboeuf, *J. Chem. Theory Comput.*, 2010, **6**, 1990–2001.
23. A. Tkatchenko, D. Alfè, and K. S. Kim, *J. Chem. Theory Comput.*, 2012, **8**, 4317–4322.
24. O. Bludský, M. Rubeš, P. Soldán, and P. Nachtigall, *J. Chem. Phys.*, 2008, **128**, 114102.
25. M. Rubeš and O. Bludský, *Chemphyschem*, 2009, **10**, 1868–1873.
26. R. M. Ferullo, N. F. Domancich, and N. J. Castellani, *Chem. Phys. Lett.*, 2010, **500**, 283–286.
27. F. Tran, J. Weber, T. a. Wesolowski, F. Cheikh, Y. Ellinger, and F. Pauzat, *J. Phys. Chem. B*, 2002, **106**, 8689–8696.
28. O. A. Vydrov and T. Van Voorhis, *J. Chem. Phys.*, 2010, **133**, 244103.
29. A. Tkatchenko, R. A. DiStasio, R. Car, and M. Scheffler, *Phys. Rev. Lett.*, 2012, **108**, 236402.
30. A. Ambrosetti, A. M. Reilly, R. A. DiStasio, and A. Tkatchenko, *J. Chem. Phys.*, 2014, **140**, 18A508.
31. W. Hujo and S. Grimme, *J. Chem. Theory Comput.*, 2011, **7**, 3866–3871.
32. S. Grimme, J. Antony, T. Schwabe, and C. Mück-Lichtenfeld, *Org. Biomol. Chem.*, 2007, **5**, 741–758.
33. T. Risthaus and S. Grimme, *J. Chem. Theory Comput.*, 2013, **9**, 1580–1591.
34. Y. Cho, S. K. Min, J. Yun, W. Y. Kim, A. Tkatchenko, and K. S. Kim, *J. Chem. Theory Comput.*, 2013, **9**, 2090–2096.

35. J. Řezáč, L. Šimová, and P. Hobza, *J. Chem. Theory Comput.*, 2013, **9**, 364–369.
36. J. Řezáč and P. Hobza, *J. Chem. Theory Comput.*, 2013, **9**, 2151–2155.
37. J. Řezáč and P. Hobza, *J. Chem. Theory Comput.*, 2014, 140625065455008.
38. O. Hübner, A. Glöss, M. Fichtner, and W. Klopper, *J. Phys. Chem. A*, 2004, **108**, 3019–3023.
39. R. J. Bartlett, J. D. Watts, S. A. Kucharski, and J. Noga, *Chem. Phys. Lett.*, 1990, **165**, 513–522.
40. K. E. Riley, M. Pitoňák, P. Jurečka, and P. Hobza, *Chem. Rev.*, 2010, **110**, 5023–5063.
41. P. Jurečka and P. Hobza, *J. Am. Chem. Soc.*, 2003, **125**, 15608–15613.
42. W. Foulkes, L. Mitas, R. Needs, and G. Rajagopal, *Rev. Mod. Phys.*, 2001, **73**, 33–83.
43. B. M. Austin, D. Y. Zubarev, and W. A. Lester, *Chem. Rev.*, 2012, **112**, 263–288.
44. J. Ma, A. Michaelides, and D. Alfè, *J. Chem. Phys.*, 2011, **134**, 134701.
45. M. Dubecký, P. Jurečka, R. Derian, P. Hobza, M. Otyepka, and L. Mitas, *J. Chem. Theory Comput.*, 2013, **9**, 4287–4292.
46. A. Ambrosetti, D. Alfè, R. A. DiStasio, and A. Tkatchenko, *J. Phys. Chem. Lett.*, 2014, **5**, 849–855.
47. P. Ganesh, J. Kim, C. Park, M. Yoon, F. A. Reboredo, and P. R. C. Kent, *J. Chem. Theory Comput.*, 2014, **10**, 5318–5323.
48. A. Halkier, T. Helgaker, P. Jørgensen, W. Klopper, and J. Olsen, *Chem. Phys. Lett.*, 1999, **302**, 437–446.
49. A. Halkier, T. Helgaker, P. Jørgensen, W. Klopper, H. Koch, J. Olsen, and A. K. Wilson, *Chem. Phys. Lett.*, 1998, **286**, 243–252.
50. P. Jurečka and P. Hobza, *Chem. Phys. Lett.*, 2002, **365**, 89–94.
51. D. G. a. Smith and K. Patkowski, *J. Chem. Theory Comput.*, 2013, **9**, 370–389.
52. TURBOMOLE V6.3, University of Karlsruhe and Forschungszentrum Karlsruhe GmbH, 1989-2007, TURBOMOLE GmbH, since 2007; available from <http://www.turbomole.com>
53. R. Ahlrichs, M. Bär, M. Häser, H. Horn, and C. Kölmel, *Chem. Phys. Lett.*, 1989, **162**, 165–169.
54. L. K. Wagner, M. Bajdich, and L. Mitas, *J. Comput. Phys.*, 2009, **228**, 3390–3404.

55. L. Horváthová, M. Dubecký, L. Mitas, and I. Štich, *Phys. Rev. Lett.*, 2012, **109**, 053001.
56. M. Korth, A. Lüchow, and S. Grimme, *J. Phys. Chem. A*, 2008, **112**, 2104–2109.
57. M. W. Schmidt, K. K. Baldridge, J. A. Boatz, S. T. Elbert, M. S. Gordon, J. H. Jensen, S. Koseki, N. Matsunaga, K. A. Nguyen, S. Su, T. L. Windus, M. Dupuis, and J. A. Montgomery, *J. Comput. Chem.*, 1993, **14**, 1347–1363.
58. M. Burkatzki, C. Filippi, and M. Dolg, *J. Chem. Phys.*, 2007, **126**, 234105.
59. M. Dubecký, R. Derian, P. Jurečka, L. Mitas, P. Hobza, and M. Otyepka, *Phys. Chem. Chem. Phys.*, 2014, **16**, 20915–20923.
60. M. Dubecký, R. Derian, P. Jurečka, L. Mitas, P. Hobza, and M. Otyepka, 2014.
61. J. Řezáč and P. Hobza, *J. Chem. Theory Comput.*, 2013, **9**, 2151–2155.
62. A. Hesselmann and G. Jansen, *Chem. Phys. Lett.*, 2002, **362**, 319–325.
63. A. Hesselmann and G. Jansen, *Chem. Phys. Lett.*, 2002, **357**, 464–470.
64. A. Hesselmann and G. Jansen, *Chem. Phys. Lett.*, 2003, **367**, 778–784.
65. A. Hesselmann, G. Jansen, and M. Schütz, *J. Chem. Phys.*, 2005, **122**, 14103.
66. H.-J. Werner, P. J. Knowles, G. Knizia, F. R. Manby, M. Schütz, and others, 2012.
67. B. Jeziorski, R. Moszynski, and K. Szalewicz, *Chem. Rev.*, 1994, **94**, 1887–1930.
68. J. P. Perdew, K. Burke, and M. Ernzerhof, *Phys. Rev. Lett.*, 1996, **77**, 3865–3868.
69. C. Adamo and V. Barone, *J. Chem. Phys.*, 1999, **110**, 6158.
70. R. van Leeuwen and E. J. Baerends, *Phys. Rev. A*, 1994, **49**, 2421–2431.
71. M. Grüning, O. V. Gritsenko, S. J. A. van Gisbergen, and E. J. Baerends, *J. Chem. Phys.*, 2001, **114**, 652.
72. J. Slater, *Phys. Rev.*, 1951, **81**, 385–390.
73. S. H. Vosko, L. Wilk, and M. Nusair, *Can. J. Phys.*, 1980, **58**, 1200–1211.
74. A. D. Becke, *Phys. Rev. A*, 1988, **38**, 3098–3100.
75. C. Lee, W. Yang, and R. G. Parr, *Phys. Rev. B*, 1988, **37**, 785–789.
76. S. Grimme, *J. Comput. Chem.*, 2006, **27**, 1787–1799.

77. J. P. Perdew, *Electronic Structure of Solids '91*, Akademie Verlag, Berlin, P. Ziesche., 1991.
78. A. D. Becke, *J. Chem. Phys.*, 1993, **98**, 5648.
79. J. Tao, J. Perdew, V. Staroverov, and G. Scuseria, *Phys. Rev. Lett.*, 2003, **91**, 146401.
80. Y. Zhao and D. G. Truhlar, *Theor. Chem. Acc.*, 2007, **120**, 215–241.
81. A. D. Becke and E. R. Johnson, *J. Chem. Phys.*, 2005, **123**, 154101.
82. E. R. Johnson and A. D. Becke, *J. Chem. Phys.*, 2006, **124**, 174104.
83. M. J. Frisch, G. W. Trucks, H. B. Schlegel, G. E. Scuseria, M. A. Robb, J. R. Cheeseman, G. Scalmani, V. Barone, B. Mennucci, G. A. Petersson, H. Nakatsuji, M. Caricato, X. Li, H. P. Hratchian, A. F. Izmaylov, J. Bloino, G. Zheng, J. L. Sonnenberg, M. Hada, M. Ehara, K. Toyota, R. Fukuda, J. Hasegawa, M. Ishida, T. Nakajima, Y. Honda, O. Kitao, H. Nakai, T. Vreven, J. A. Montgomery Jr., J. E. Peralta, F. Ogliaro, M. Bearpark, J. J. Heyd, E. Brothers, K. N. Kudin, V. N. Staroverov, R. Kobayashi, J. Normand, K. Raghavachari, A. Rendell, J. C. Burant, S. S. Iyengar, J. Tomasi, M. Cossi, N. Rega, J. M. Millam, M. Klene, J. E. Knox, J. B. Cross, V. Bakken, C. Adamo, J. Jaramillo, R. Gomperts, R. E. Stratmann, O. Yazyev, A. J. Austin, R. Cammi, C. Pomelli, J. W. Ochterski, R. L. Martin, K. Morokuma, V. G. Zakrzewski, G. A. Voth, P. Salvador, J. J. Dannenberg, S. Dapprich, A. D. Daniels, Ö. Farkas, J. B. Foresman, J. V. Ortiz, J. Cioslowski, and D. J. Fox, Gaussian, Inc., Wallingford CT, 2009.
84. V. Blum, R. Gehrke, F. Hanke, P. Havu, V. Havu, X. Ren, K. Reuter, and M. Scheffler, *Comput. Phys. Commun.*, 2009, **180**, 2175–2196.
85. Y. Shao, L. F. Molnar, Y. Jung, J. Kussmann, C. Ochsenfeld, S. T. Brown, A. T. B. Gilbert, L. V. Slipchenko, S. V. Levchenko, D. P. O'Neill, R. A. DiStasio, R. C. Lochan, T. Wang, G. J. O. Beran, N. A. Besley, J. M. Herbert, C. Y. Lin, T. Van Voorhis, S. H. Chien, A. Sodt, R. P. Steele, V. A. Rassolov, P. E. Maslen, P. P. Korambath, R. D. Adamson, B. Austin, J. Baker, E. F. C. Byrd, H. Dachsel, R. J. Doerksen, A. Dreuw, B. D. Dunietz, A. D. Dutoi, T. R. Furlani, S. R. Gwaltney, A. Heyden, S. Hirata, C.-P. Hsu, G. Kedziora, R. Z. Khalliulin, P. Klunzinger, A. M. Lee, M. S. Lee, W. Liang, I. Lotan, N. Nair, B. Peters, E. I. Proynov, P. A. Pieniazek, Y. M. Rhee, J. Ritchie, E. Rosta, C. D. Sherrill, A. C. Simmonett, J. E. Subotnik, H. L. Woodcock, W. Zhang, A. T. Bell, A. K. Chakraborty, D. M. Chipman, F. J. Keil, A. Warshel, W. J. Hehre, H. F. Schaefer, J. Kong, A. I. Krylov, P. M. W. Gill, and M. Head-Gordon, *Phys. Chem. Chem. Phys.*, 2006, **8**, 3172–3191.
86. G. Kresse and J. Furthmüller, *Phys. Rev. B. Condens. Matter*, 1996, **54**, 11169–11186.
87. K. Lee, É. D. Murray, L. Kong, B. I. Lundqvist, and D. C. Langreth, *Phys. Rev. B*, 2010, **82**, 081101.
88. J. Klimeš, D. R. Bowler, and A. Michaelides, *J. Phys. Condens. Matter*, 2010, **22**, 022201.

89. P. Lazar, F. Karlický, P. Jurečka, M. Kocman, E. Otyepková, K. Šafářová, and M. Otyepka, *J. Am. Chem. Soc.*, 2013, **135**, 6372–6377.
90. J. Antony and S. Grimme, *Phys. Chem. Chem. Phys.*, 2008, **10**, 2722–2729.
91. R. C. Lochan and M. Head-Gordon, *Phys. Chem. Chem. Phys.*, 2006, **8**, 1357–1370.
92. M. Kocman, M. Pykal, and P. Jurečka, *Phys. Chem. Chem. Phys.*, 2014, **16**, 3144–3152.
93. V. Spirko, M. Rubeš, and O. Bludský, *J. Chem. Phys.*, 2010, **132**, 194708.
94. L. Mattera, F. Rosatelli, C. Salvo, F. Tommasini, U. Valbusa, and G. Vidali, *Surf. Sci.*, 1980, **93**, 515–525.
95. E. Ghio, L. Mattera, C. Salvo, F. Tommasini, and U. Valbusa, *J. Chem. Phys.*, 1980, **73**, 556.
96. S. Grimme, C. Mück-Lichtenfeld, and J. Antony, *J. Phys. Chem. C*, 2007, **111**, 11199–11207.
97. Y. Zhang, W. Pan, and W. Yang, *J. Chem. Phys.*, 1997, **107**, 7921–7925.
98. S. N. Steinmann, C. Piemontesi, A. Delachat, and C. Corminboeuf, *J. Chem. Theory Comput.*, 2012, **8**, 1629–1640.
99. V. V Gobre and A. Tkatchenko, *Nat. Commun.*, 2013, **4**, 2341.
100. O. A. von Lilienfeld and A. Tkatchenko, *J. Chem. Phys.*, 2010, **132**, 234109.